

See discussions, stats, and author profiles for this publication at: <https://www.researchgate.net/publication/263955099>

# Surface Modification of Membrane Filters Using Graphene and Graphene Oxide-Based Nanomaterials for Bacterial Inactivation and Removal

ARTICLE *in* ACS SUSTAINABLE CHEMISTRY & ENGINEERING · APRIL 2014

Impact Factor: 4.64 · DOI: 10.1021/sc500044p

---

CITATIONS

10

---

READS

101

## 4 AUTHORS, INCLUDING:



Debora F Rodrigues

University of Houston

43 PUBLICATIONS 1,208 CITATIONS

SEE PROFILE

## Surface Modification of Membrane Filters Using Graphene and Graphene Oxide-Based Nanomaterials for Bacterial Inactivation and Removal

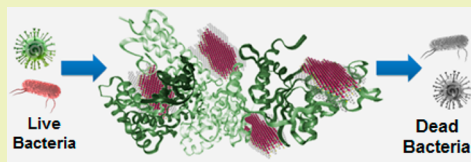
Yvonne Ligaya F. Musico,<sup>†,‡</sup> Catherine M. Santos,<sup>†</sup> Maria Lourdes P. Dalida,<sup>‡</sup> and Debora F. Rodrigues<sup>\*,†</sup>

<sup>†</sup>Department of Civil and Environmental Engineering, University of Houston, Houston, Texas 77204-5003, United States

<sup>‡</sup>Environmental Engineering Graduate Program, College of Engineering, University of the Philippines, Diliman, Quezon City 1101, Philippines

**ABSTRACT:** Surfaces of commercially available membrane filters were modified by the dispersion of poly(*N*-vinylcarbazole) (PVK), graphene (G), poly(*N*-vinylcarbazole)-graphene (PVK-G), graphene oxide (GO), and poly(*N*-vinylcarbazole)-graphene oxide (PVK-GO) in order to impart antibacterial properties. The successful coatings of the membranes were demonstrated through scanning electron microscopy (SEM) and Fourier transform infrared (FT-IR) spectroscopy. Investigations carried out on the surface-modified membrane filters using *Escherichia coli* and *Bacillus subtilis* showed that the presence of graphene-based nanomaterials significantly improved the antibacterial properties of the membrane filters. One of the mechanisms for this improved antimicrobial property of the filter was attributed to the production of reactive oxygen species by the nanomaterials. Among the nanomaterials used in this study, the PVK-GO-modified membrane filter exhibited the best removal of *B. subtilis* and *E. coli* with 4 and 3 log removals, respectively. The different levels of *E. coli* and *B. subtilis* removals were attributed to the differences in their cell structures and composition. This study has demonstrated that the use of graphene-based nanomaterials to modify the surfaces of membrane filters is an effective method of imparting antibacterial properties that can find useful application in water and wastewater treatment.

**KEYWORDS:** Antibacterial, Graphene-based nanocomposites, Membrane filter, PVK-GO



### INTRODUCTION

Microbial contamination of drinking water contributes to disease outbreaks and background rates of disease in developing and developed countries.<sup>1,2</sup> Waterborne pathogens, including bacteria, protozoans, helminthes, fungi, and viruses cause more than 3 million deaths and innumerable cases of sickness every year.<sup>3</sup> To protect public health from pathogens, water disinfection and microbial control should be given important attention.<sup>3,4</sup> Some conventional ways to remove pathogenic bacteria include chemical treatment (e.g., chlorination, ozonation), ultraviolet (UV) treatment, and thermal treatment (heating).<sup>5</sup> Chemical agents (such as chlorine and its compounds) are most widely used because of their effectiveness and low cost.<sup>3</sup> However, chemical disinfectants can react with various constituents in natural water to form disinfection byproducts (DBPs), many of which are carcinogens.<sup>3,4</sup> Moreover, some pathogens are resistant to conventional disinfectants that require extremely high dosages leading to aggravated DBP formation.<sup>4</sup>

In recent years, membrane technologies have been favored over other technologies for water treatment, such as disinfection, distillation, or media filtration, because they do not require additives, thermal inputs, or require regeneration of spent media.<sup>6,7</sup> Membrane technologies are commercially available for various water and wastewater treatments, including bacterial removal.<sup>6</sup> Performance of the membranes depends

largely on the properties of their surfaces; hence, much attention has been paid to membrane surface modifications.<sup>8,9</sup>

Studies have shown that functionalization of membrane surfaces with nanoparticles is one way to improve membrane performance.<sup>10–12</sup> Recently, graphene-based polymer nanocomposites have been shown to combine unique features of graphene-based nanoparticles and polymer materials in one nanohybrid material.<sup>13</sup> These nanohybrid materials have properties that cannot be achieved using conventional composites or virgin polymers.<sup>14</sup> One very promising nanohybrid material is the poly(*N*-vinylcarbazole) (PVK) containing carbon-based nanomaterials, such as graphene oxide (GO), graphene (G), and single-walled carbon nanotubes (SWNTs).<sup>15–17</sup> Among the PVK nanocomposites, PVK-GO and PVK-G seems the most promising. These nanocomposites have significant antimicrobial properties<sup>17,18</sup> and do not present mammalian cell cytotoxicity.<sup>17</sup> These properties of PVK-G and PVK-GO polymer graphene-based composites suggest that these nanocomposites can be used to improve the functions of membrane filters for water and wastewater treatment.

**Special Issue:** Sustainable Nanotechnology 2013

**Received:** January 21, 2014

**Revised:** April 7, 2014

**Published:** April 8, 2014

In the present study, the development and performance of membrane filters modified with PVK-GO and PVK-G were compared to membranes modified with only PVK, G, or GO. The antibacterial properties of these graphene-based nanocomposite-modified membrane filters were investigated. The results showed that graphene-based nanocomposite-modified membrane filters have improved the antibacterial properties. Among these graphene-based nanocomposite-modified membrane filters, PVK-GO-modified membrane filters exhibited a better antibacterial property than other modified and non-modified membranes.

## MATERIALS AND METHODS

**Materials.** Graphene nanoplatelets (GNP) were purchased from XG Sciences, MI, while the poly(*N*-vinylcarbazole) (PVK) was obtained from Sigma-Aldrich (U.S.A.). Some reagents such as  $H_2SO_4$ , HCl, and  $KMnO_4$  were purchased from Fisher Scientific.  $H_2O_2$  was obtained from Macron. The  $NaNO_3$  and NaOH were purchased from Merck KGaA and Across, respectively. Tryptic soy agar (TSA), tryptic soy broth (TSB), and phosphate buffer saline (PBS) were obtained from Becton Dickinson (U.S.A.). The membrane used for antimicrobial properties evaluation was 8.0  $\mu\text{m}$  pore size cellulose nitrate membrane filters (Whatman, 47 mm diameter). The large pore size membrane filters were used in this study to reduce the sieving effect of the membrane pores to allow determination of the role of graphene-based nanomaterials coatings in the inactivation and removal of microorganisms. All chemical reagents were of analytical grade and used without further purification. The aqueous solutions were prepared using deionized (DI) water.

**GO Synthesis.** The GO was prepared using the modified Hummers' method.<sup>19</sup> Briefly, 3 g of graphene nanoplatelets (GNP) were mixed with 3 g of  $NaNO_3$  and then dispersed in 138 mL of  $H_2SO_4$  in an ice bath for 30 min. The mixture was then oxidized by adding 18 g of  $KMnO_4$  and stirred for another 30 min in the ice bath. The temperature was then increased and maintained at  $35 \pm 5^\circ\text{C}$  for 24 h to complete the graphite oxidation. After 24 h of oxidation, 240 mL of water was added with continuous stirring for 30 min at  $90 \pm 5^\circ\text{C}$ . The mixture was further diluted with 600 mL of water and stirred continuously for 10 min at  $90 \pm 5^\circ\text{C}$ . After which, 18 mL of  $H_2O_2$  was added, and then the solution was cooled to room temperature. The product was centrifuged at 10,000 rpm for 10 min, and the pellets were collected. The solids were washed with base (1.0 M NaOH) and acid (1.0 M HCl) for 30 min each. After the base and acid washings, water washings were done to neutralize the pH of the final product. The residue was then washed with methanol and bath sonicated for 1 h. Finally, the product was dried overnight in a vacuum oven at  $40^\circ\text{C}$ .

**Preparation of PVK-GO and PVK-Graphene (PVK-G).** The PVK-GO and PVK-G nanocomposite solutions were prepared by dispersing 20 mg of GNP or GO powder in 20 mL of DI water to make 1 mg/mL solution followed by sonication for 30 min as previously described.<sup>16,17</sup> Briefly, the PVK solution (1 mg/mL) was prepared by dissolving 5 mg of PVK powder in 1 mL 1-cyclohexyl-2-pyrrolidone (CHP) solution followed by ultrasonication for 6 h and addition of 4 mL of DI water. The PVK-GO and PVK-G solutions were prepared by a mixing process. The PVK solution was slowly mixed into the GO or G solution at 10:90 wt % concentration ratio, and then the mixture was ultrasonicated for another 30 min prior to use.

**Modification of Membrane Filters.** The commercially available cellulose nitrate membrane filters of 8.0  $\mu\text{m}$  pore size (Whatman, 47 mm diameter) were modified by dispersing 3.0 mL of the nanomaterial solution (1 mg/mL) on the surface of the filter using a vacuum filter. The modified nanocomposite membrane filters were air-dried overnight and washed with DI water prior to use.

**Characterization of Nanomaterials and Nanocomposites.** Fourier transform infrared (FT-IR) spectroscopy and scanning electron microscopy (SEM) were used to characterize the successful coating, chemical composition, and functional groups of the

nanomaterials and nanocomposites on the membrane filters. Attenuated total reflectance infrared (ATR-IR) measurements were performed using a Nicolet iS10 mid infrared FT-IR spectrometer (Thermo Fisher Scientific) equipped with ZnSe crystals. Data were acquired using the Omnic 8 Software (Thermo Fisher Scientific). The SEM images were acquired using a JSM-6010LA InTouch scope (JEOL, U.S.A.) equipped with energy dispersive spectroscopy (EDS) with the latest silicon drift detector (SDD) for elemental analysis. All experiments were done in triplicate.

**Filtration Assay for Antimicrobial Analyses.** Single isolated colonies of *Escherichia coli* K12 MG1655 (ATCC 700926) and *Bacillus subtilis* (ATCC 6633) were inoculated and incubated overnight in tubes with 5 mL TSB at  $37^\circ\text{C}$ . After that, the bacterial cultures were centrifuged at 10,000 rpm for 10 min. The supernatant was decanted, while the bacterial pellets were washed twice and suspended in PBS to prepare a bacterial solution with optical density (OD) of 0.5 at 600 nm wavelength.

All apparatus and equipment used in this experiment were autoclaved prior to filtration, and the experiments were done aseptically in a biosafety cabinet. A 3 mL volume of bacterial solutions containing either *E. coli* or *B. subtilis* were passed through the modified membrane filters by gravity filtration. This filtration method was also done in parallel with control unmodified filters. All samples were done in triplicate. Bacterial analyses were done on the filter surfaces and flow through solution. For the surface filter analyses, filters were subjected to the filter agar test and scanning electron microscopy (SEM).

**Regrow Assay of Bacteria Retained on the Filter.** The viability and regrowth potential of the retained bacterial cells on the membrane surfaces were tested using the filter agar assay.<sup>15</sup> Immediately after filtration, the filter surfaces were flipped on a TSA plate facing down and incubated overnight at  $37^\circ\text{C}$ . Bacterial growth on the membrane perimeter was measured with a Mitutoyo 500-196-20 digital micrometer calliper (MSI Viking Gage, U.S.A.). Averages and standard deviations were calculated from triplicates.

**Scanning Electron Microscopy (SEM) Imaging of the Membrane Surface.** For the SEM sample preparation and imaging after the filtration assays, the bacterial cells on the filter surfaces were fixed with 2% glutaraldehyde in a 0.05 M cacodylate buffer solution (Fisher Scientific, U.S.A.) as previously described.<sup>15</sup> The fixed cells were subsequently stained with 1% osmium tetroxide (Sigma-Aldrich Chemicals, U.S.A.) and dehydrated with increasing concentrations of ethanol (25%, 50%, 75%, 95%, and 100%). SEM images were acquired using a JSM-6010LA InTouch scope (JEOL, USA) equipped with energy dispersive spectroscopy (EDS) with the latest silicon drift detector (SDD) for elemental analysis.

**Quantification of Microbial Removal in the Filtrate.** Viable bacteria were enumerated in the flow through solution using the plate count method.<sup>20</sup> The filtrates were collected and diluted in PBS through serial dilutions. The dilutions were plated on TSA (Oxoid, England) media and incubated overnight at  $37^\circ\text{C}$ . The total number of colony-forming units (CFU/mL) was determined. Each filtrate sample was plated in duplicate, and standard deviations were calculated from the triplicate assays.

**Measurement of Release of Intracellular Material.** The DNA concentration ( $\text{ng}/\mu\text{L}$ ) in the flow through was also analyzed to determine release of intracellular material from damaged bacterial cells after filtration. The experimental procedure was adapted from a previously described method.<sup>21</sup> Briefly, immediately after filtration, 2  $\mu\text{L}$  of the filtrates were placed in a Take 3 Plate (for DNA quantification) in the Synergy MX (BioTek, U.S.A.). Sterile PBS without bacteria and DNA were used as blanks. Average DNA concentrations and standard deviations were calculated from triplicate filtrate samples.

**Metabolic Activity of Microorganisms Exposed to Nanomaterials and Nanocomposites.** The antibacterial properties of nanomaterials used to modify commercial membrane filters were evaluated by metabolic assay test using a Vybrant cell metabolic assay kit (Molecular Probes) prior to the membrane coating. This was done by adding 180  $\mu\text{L}$  of bacterial solution to 20  $\mu\text{L}$  of the nanomaterial solution in a 96-well clear bottom black plate (Corning, VWR). The

bacterial–nanomaterial mixtures were prepared in triplicate. A mixture of 20  $\mu\text{L}$  of DI water and 180  $\mu\text{L}$  of bacterial solution was used as a positive control sample, and a solution of 180  $\mu\text{L}$  of DI water with 20  $\mu\text{L}$  of nanomaterials/nanocomposites was used as a negative control. The bacterial–nanomaterial mixtures were incubated at 37 °C and 50 rpm for 1 h. After 1 h of incubation, 10  $\mu\text{L}$  of C12-resazurin (10  $\mu\text{M}$ ) was added to each well and incubated for another 15 min at 37 °C. The bacterial viability was monitored using a Synergy MX microtiter plate reader (Biotek) by measuring the fluorescence intensity of the resorufin product at 587 nm. The percentage of metabolic active cells was calculated by getting the ratio of the fluorescence intensity acquired for the bacteria exposed to each nanomaterial to the fluorescence intensity of the control and then multiplying by 100. The standard deviations were based on triplicate assays.

**Reactive Oxygen Species Assay.** The concentration of thiols in glutathione (GSH) was quantified by Ellman's assay.<sup>22,23</sup> This was performed by adding 225  $\mu\text{L}$  of graphene, GO, PVK, PVK-G, or PVK-GO nanomaterial solution (1 mg/mL) in 50 mM NaHCO<sub>3</sub> (pH 8.6) into 225  $\mu\text{L}$  of GSH (0.8 mM in bicarbonate buffer). The GSH (0.4 mM) oxidized in H<sub>2</sub>O<sub>2</sub> (1 mM) was used as positive control, while the GSH solution without nanomaterials was used as negative control. All samples were done in triplicate. The mixtures were placed in a 2 mL eppendorf tube, covered with aluminum foil (to prevent illumination), and then incubated in a shaker with a speed of 150 rpm at 30 ± 5 °C for 2 h. After incubation, 785  $\mu\text{L}$  of 0.05 mM Tris-HCl and 15  $\mu\text{L}$  DNTB ((Ellman's reagent, 5,5'-dithio-bis(2-nitrobenzoic acid), Sigma-Aldrich) were added to bring out the yellow color in the product. The nanomaterials were filtered out from the solution using a 33 mm diameter and 0.45  $\mu\text{m}$  pore size poly(ether sulfone) (PES) Millex syringe filter. A 250  $\mu\text{L}$  aliquot of filtrate from each sample was transferred into a black 96-well plate. The absorbance was then measured at 412 nm using a Synergy MX microtiter plate reader (Biotek). The GSH loss was calculated using the following formula

$$\begin{aligned} \text{\% GSH loss} \\ = \frac{(\text{absorbance of negative control} - \text{absorbance of sample})}{\text{absorbance of negative sample}} \\ \times 100 \end{aligned}$$

## RESULTS AND DISCUSSION

**Characterization of Nanomaterials and Nanocomposites Coated Filters.** The newly synthesized nanocomposites filters were characterized to determine their successful preparation. FT-IR was employed to identify the functional groups present in the nanomaterials and nanocomposites. The PVK (Figure 1c) was found to have the following characteristic peaks: 745  $\text{cm}^{-1}$  (aromatic C–H bend), 1330  $\text{cm}^{-1}$  (C–N stretch from vinylcarbazole), 1670  $\text{cm}^{-1}$  (C=C stretch), 2930  $\text{cm}^{-1}$  (aliphatic C–H stretch from the polymer backbone), and 3100  $\text{cm}^{-1}$  (aromatic C–H stretch). The above-mentioned absorption peaks are also shown in both PVK-G (Figure 1b) and PVK-GO (Figure 1d) with additional peaks positioned at 1060  $\text{cm}^{-1}$  (C–O carbonyl stretching of carboxylic acid) and 1610  $\text{cm}^{-1}$  (C=O carbonyl stretching of carboxylic acid). These additional distinguishing peaks were also characteristic for graphene (Figure 1a) and GO (Figure 1e). Moreover, a distinctive and significant peak located at 3350  $\text{cm}^{-1}$  that corresponds to broad O–H stretching of the carboxylic acid/hydroxyl group was observed for GO and PVK-GO. These FT-IR absorption characteristics show the successful preparation of the nanocomposites.<sup>24</sup>

**Microbial Removal by Modified Membrane Filters. Effects of Nanomaterials and Nanocomposites on Membrane Filters.** To investigate the successful incorporation of nanomaterials in the membrane filters and to understand the

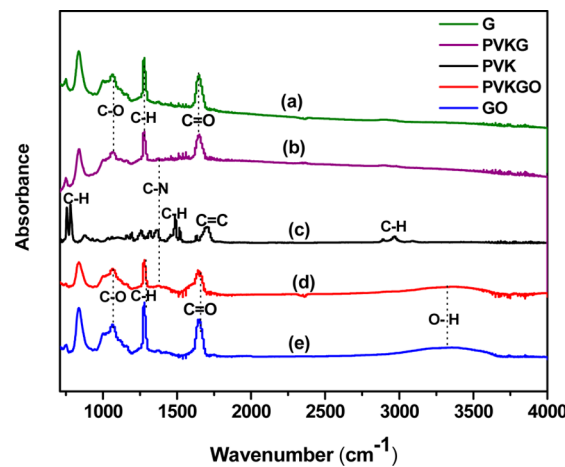


**Figure 1.** FT-IR of nanomaterials (a) G, (b) PVK-G, (c) PVK, (d) PVK-GO, and (e) GO with their representative peaks.

interaction of the nanomaterials with bacteria, the surface morphologies of unmodified and modified membrane filters before and after filtration were examined using SEM. The scanned images show the successful coating of the filter surfaces with PVK (Figure 2c), G (Figure 2e), PVK-G (Figure 2g), GO

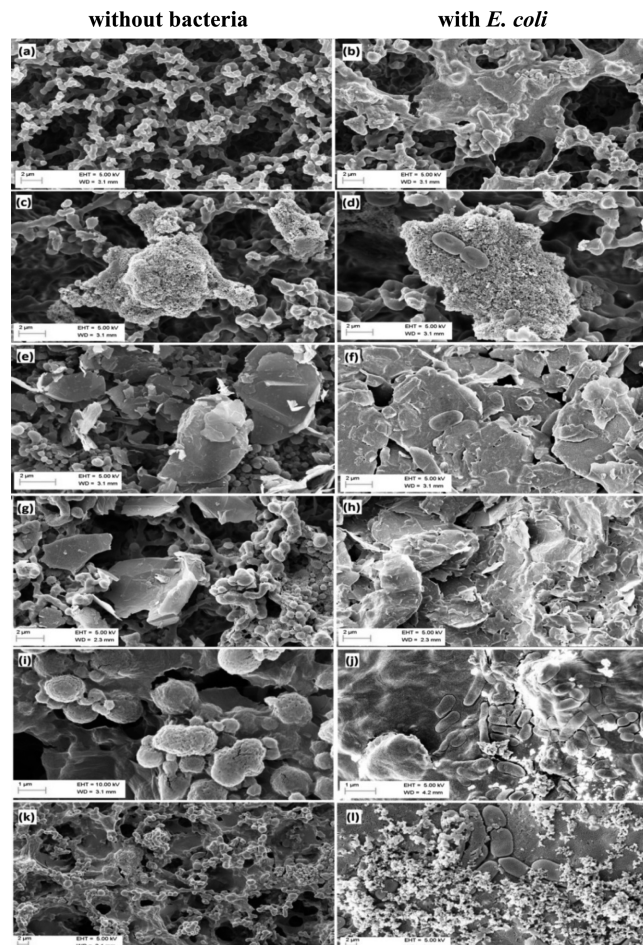


**Figure 2.** SEM of (a,b) cellulose nitrate filters, (c,d) PVK coated membranes, (e,f) graphene coated membranes, (g,h) PVK-G nanocomposite coated membranes, (i,j) GO coated membranes, and (k,l) PVK-GO nanocomposite coated membranes.

(Figure 2i), and PVK-GO (Figure 2k). Representative SEM images of the filters after coating show that the coating of the membranes with G, GO, PVK-G, and PVK-GO reduces the pore size of the membrane, leading to an increase in retention of bacteria compared to unmodified and PVK-modified membrane filters (Figure 2).

The cells retained on the filters containing GO, G, PVK-GO, and PVK-G show a flattened aspect characteristic of cells losing their integrity when compared to the cells deposited on uncoated membranes or containing only PVK. This observation corroborates previous antimicrobial studies that demonstrated that these nanomaterials and nanocomposites present antimicrobial activities.<sup>23,25,26</sup>

The viability and potential regrowth of bacteria retained on the filter surface was further evaluated by the filter agar assay. The results depicted in Figure 3 show that modified membrane

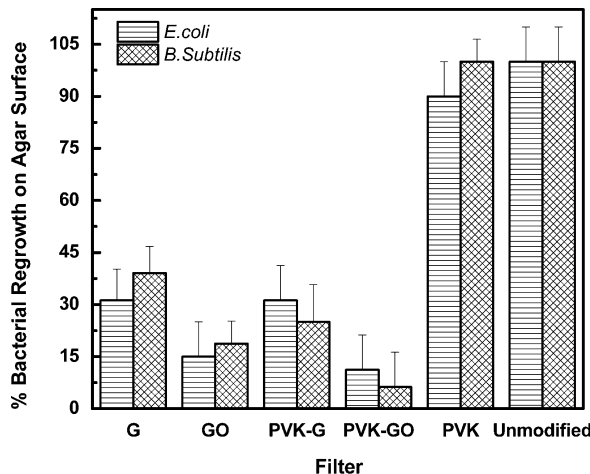


**Figure 3.** Agar printing assay showing percentage of bacterial regrowth to determine the growth behavior of bacteria retained on membranes coated with G, GO, PVK-G, PVK-G, and PVK and unmodified membranes. The data was normalized based on the controls. Concentration of nanomaterial and nanocomposite solutions used to coat the filters: 1 mg/mL. Error bars indicate the standard deviation of triplicate measurements.

filters with GO, G, PVK-G, and PVK-GO present a reduced bacterial growth compared to PVK-modified and unmodified membrane filters. The results also show that *E. coli* (Gram-negative) exhibited more reduced, even though it was not statistically significant, bacterial growth than *B. subtilis* (Gram-positive) in the presence of the pristine nanomaterials GO and G, while the opposite was observed with the nanocomposites containing PVK. This difference in response of different bacteria to various carbon-based nanomaterials<sup>25,27,28</sup> and metal oxide nanoparticles<sup>29</sup> was also observed in previous studies.

**Microbial Removal in the Filtrate.** To estimate the effectiveness of the membranes in removing bacteria from an aqueous solution, bacterial plate counts were conducted with the filtrates. The results depicted in Figure 4 show that both GO and PVK-GO plate counts present a removal of 4 and 3 logs for *B. subtilis* and *E. coli*, respectively. This bacterial removal might be a combined effect of cell retention and inactivation by GO and G while passing through the membranes. The reduced pore size generated by these nanocomposites, the added thickness of GO, G, PVK-G, and PVK-GO layers to the membrane, and the strong antimicrobial

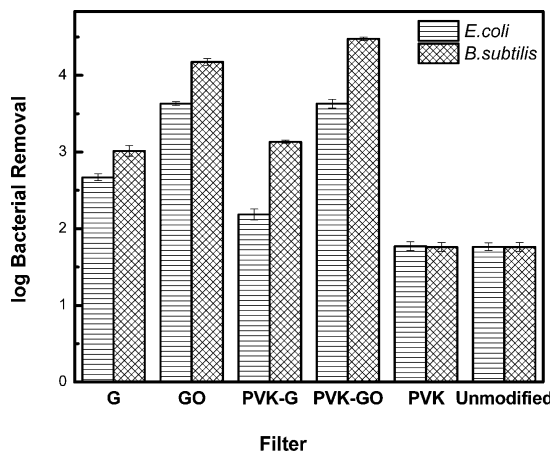


**Figure 4.** Log bacterial removal after filtration through nanocomposite membrane filter. Concentration of nanomaterial solution on filter: 1 mg/mL. Error bars indicate the standard deviation of triplicate measurements.

activity of the nanomaterials increased the efficiency of the filters by cell inactivation, sieving, and depth filtration mechanisms.<sup>21,30,31</sup> This result is consistent with the filter agar test result of this study, wherein GO, G, PVK-G, and PVK-GO presented higher inactivation of bacterial cells than the unmodified and PVK-modified membranes. Furthermore, the removal of *B. subtilis* cells during the filtration was slightly higher than *E. coli*. Although this difference in levels of tolerance by different microorganisms to carbon-based nanomaterials was not thoroughly studied, this antimicrobial activity is tentatively attributed to differences in the bacterial cell structures.<sup>28</sup> Gram-negative bacteria have much thinner cell walls made of peptidoglycan and an external lipid membrane. The Gram-positive bacteria, on the other hand, have thicker peptidoglycan cell walls but no external lipid membrane. The fact that some carbon-based nanomaterials tend to be more hydrophobic facilitates their partition into the lipid membrane of Gram-negative bacteria. It is possible that the addition of PVK reduces the hydrophobicity of the nanomaterials, which would explain the increase inactivation of Gram-positive bacteria that do not have an external lipid bilayer. The difference observed between GO/PVK-GO and G/PVK-G bacterial inactivation is also clear in Figure 3. However, the potential mechanisms of inactivation are discussed later in the Reactive Oxygen Species Production section.

The results obtained from the SEM images (Figure 2) suggested that there is cell membrane damage. Therefore, the bacterial inactivation by modified and unmodified membrane filters was further evaluated by measuring the efflux of cytoplasmic material (e.g., DNA) in the filtrate. Current literature describes that the release of large quantities of intracellular material from cells only occurs when bacterial cell walls and cellular membranes suffer irreparable damages.<sup>21</sup> The results in Figure 5 show that the PVK-GO-modified membrane filter had the highest increase in bacterial DNA release for both *E. coli* and *B. subtilis* bacteria. The DNA quantification result corroborates the plate count analyses of the filtrate, confirming that GO- and PVK-GO-modified membrane filters have better antimicrobial activity compared to the other nanomaterials used in this study.

**Antimicrobial Mechanisms of Nanomaterials. Microbial Metabolic Activity in Presence of Nanomaterials.** The

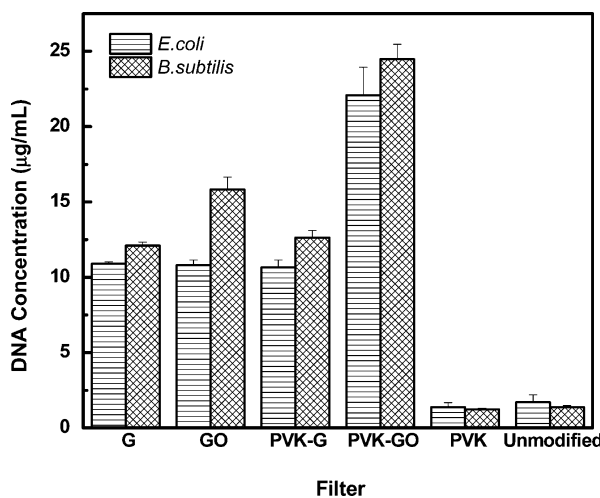


**Figure 5.** DNA concentration in the filtrate after filtration through nanocomposite membrane filter. Concentration of nanomaterial solution on filter: 1 mg/mL. Error bars indicate the standard deviation of triplicate measurements.

metabolic assays were done to determine the potential antibacterial properties of the newly synthesized nanomaterials. The results show that bacteria exposed to graphene, GO, PVK-G, and PVK-GO nanomaterial solutions were less metabolically active than the bacteria exposed to PVK only (Figure 6).

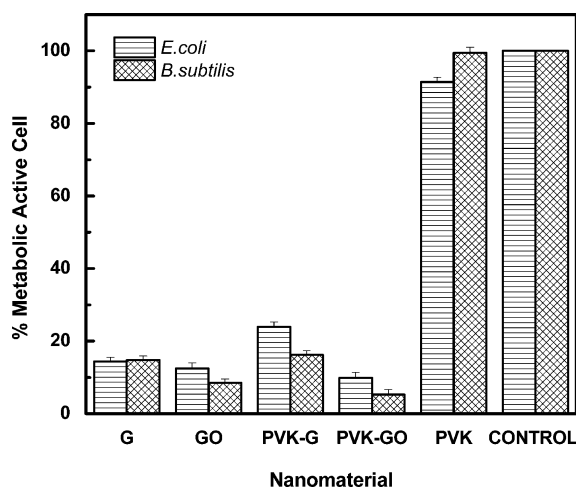


**Figure 6.** Percentage of metabolic active cells after exposure to each nanocomposite. Nanomaterial solution concentration: 1 mg/mL. The control sample did not contain any nanomaterial. Error bars indicate the standard deviation of triplicate measurements.

Among the nanomaterials and nanocomposites investigated, PVK-GO inhibited the most the metabolic activity of both *E. coli* and *B. subtilis*, while PVK presented a similar trend to the control. This suggests that the PVK-GO nanocomposite has better antimicrobial activity than the other nanomaterials used in this study. The results also show that PVK had a negligible antibacterial activity but enhanced the antimicrobial properties of graphene and GO. This improvement in antimicrobial activity was previously observed and reported for other ratios of PVK-G,<sup>32</sup> PVK-GO,<sup>17</sup> and PVK-SWNT<sup>33</sup> nanocomposites. It is worth noting that the presence of PVK in the nanocomposite did not hinder the known antibacterial properties of G and GO but rather enhanced their bactericidal properties. This

improved antibacterial activity of the nanocomposite was described to be related to a better dispersion of G and GO in the presence of PVK through  $\pi-\pi$  stacking interactions between the carbazole group of PVK and the aromatic groups present in the carbon nanomaterials.<sup>32</sup> This better dispersion leads to a greater contact between the cells and nanomaterials, therefore leading to greater cell damage.<sup>16</sup>

**Reactive Oxygen Species Production.** Carbon-based nanomaterials have been described to produce reactive oxygen species (ROS) that can cause cellular damage and death through oxidative stress.<sup>21,23</sup> In order to investigate the production of ROS by this new nanocomposite, an oxidative stress assay was performed with these nanomaterials (Figure 7).

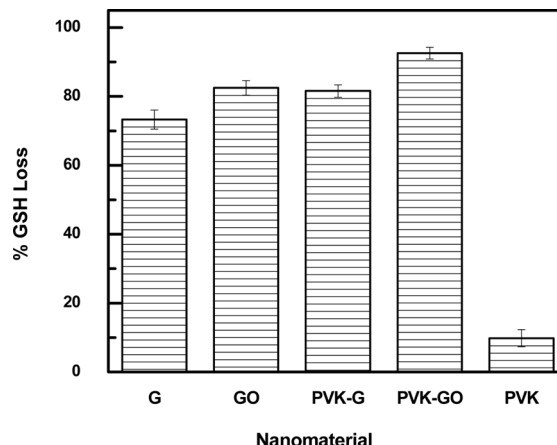


**Figure 7.** Quantification of loss of total glutathione (GSH) after 2 h exposure to each nanomaterial. This assay aims to assess toxicological responses that can promote oxidative stress. Nanomaterial solution concentration: 1 mg/mL. Error bars indicate standard deviation of triplicate measurements.

This assay involves the measurement of the percentage loss of total glutathione (GSH). GSH is an important molecule protecting mammalian cells from toxic compounds;<sup>34</sup> hence, GSH loss means the presence of oxidative species that can cause bacterial cell death. In Figure 7 the PVK-GO nanocomposite exhibits the highest percentage of GSH loss, thus indicating high production of reactive oxygen species that leads to more oxidative stress to the bacteria. The percent loss of GSH was calculated and determined to be statistically different from the control by *t*-test analyses.

Our results also show that graphene oxide (GO) produced more ROS than graphene. This higher production of ROS by GO can be attributed to the larger number of oxygen-containing functional groups, such as  $-\text{COOH}$  and  $\text{OH}^-$  in GO as shown in Figure 1, that could facilitate the production of reactive oxygen species. This result corroborates well the metabolic activity assay results (Figure 6). Furthermore, these results suggest that the antibacterial property of the nanomaterials is related to oxidative stress generation, which interferes with the bacterial metabolic activity and leads to cellular inactivation.<sup>35</sup>

## CONCLUSION

The coating of membrane filters with graphene-based nanomaterials can significantly improve the antibacterial properties of commercial membrane filters. The antibacterial assays on modified membrane filters and filtrates suggest that the

mechanism of inactivation of bacterial cells by graphene-based nanomaterials were ROS and inhibition of bacterial growth by damaging the cells and interfering in the bacterial metabolic activity. The different levels of tolerance to the nanomaterials and nanocomposites observed between *E. coli* (Gram-negative) and *B. subtilis* (Gram-positive) can be attributed to the difference in their cell wall structures and compositions. Among the graphene-based modified membrane filters used in this study, PVK-GO was the most promising because it consistently exhibited the best antimicrobial property. The results show that surface modification of membrane filters with graphene-based nanomaterials enhanced the antibacterial properties of membrane filters that can be applied for water and wastewater treatment.

## AUTHOR INFORMATION

### Corresponding Author

\*E-mail: dfrigirodrigues@uh.edu

### Notes

The authors declare no competing financial interest.

## ACKNOWLEDGMENTS

This research project was partially funded by the University of Houston New Faculty Research Program, Award #102556, Research Experience for Teachers (RET) program (NSF Award #1130006), and National Science Foundation Career Award (NSF Award #150255). We acknowledge the Department of Science and Technology – Engineering Research and Development for Technology (DOST-ERDT) program at the University of the Philippines that provided a one year scholarship to Yvonne L. F. Musico to conduct this investigation at the University of Houston. We also thank Ms. Ashley Buhring (high school teacher) for helping out with the sample processing and analyses during the summer of 2012.

## REFERENCES

- (1) LeChevallier, M. A. K. Water Treatment and Pathogen Control: Process Efficiency in Achieving Safe Drinking Water. WHO, IWA Publishing: London, 2004.
- (2) Cabral, J. P. S. Water microbiology. Bacterial pathogens and water. *Int. J. Environ. Res. Public Health* **2010**, *7* (10), 3657–3703.
- (3) Seo, Y. I.; Hong, K. H.; Kim, S. H.; Chang, D.; Lee, K. H.; Kim, Y. D. Removal of bacterial pathogen from wastewater using Al filter with Ag-containing nanocomposite film by in situ dispersion involving polyol process. *J. Hazard. Mater.* **2012**, *227–228* (0), 469–473.
- (4) Li, Q.; Mahendra, S.; Lyon, D. Y.; Brunet, L.; Liga, M. V.; Li, D.; Alvarez, P. J. J. Antimicrobial nanomaterials for water disinfection and microbial control: Potential applications and implications. *Water Res.* **2008**, *42* (18), 4591–4602.
- (5) Haas, C. N.; Hutzler, N. J. Wastewater disinfection and infectious disease risks. *Crit. Rev. Environ. Control* **1986**, *17* (1), 1–20.
- (6) Pendergast, M. M.; Hoek, E. M. V. A review of water treatment membrane nanotechnologies. *Energy Environ. Sci.* **2011**, *4* (6), 1946–1971.
- (7) Ulbricht, M. Advanced functional polymer membranes. *Polymer* **2006**, *47* (7), 2217–2262.
- (8) Khulbe, K. C.; Feng, C.; Matsuura, T. The art of surface modification of synthetic polymeric membranes. *J. Appl. Polym. Sci.* **2010**, *115* (2), 855–895.
- (9) Brady-Estevez, A. S.; Kang, S.; Elimelech, M. A single-walled-carbon-nanotube filter for removal of viral and bacterial pathogens. *Small* **2008**, *4* (4), 481–484.
- (10) Muller, N.; Crawley, T. Nanoenhanced Membranes for Improved Water Treatment. *ObservatoryNano Briefing No. 16*; June 15, 2011.
- (11) Kim, E.-S.; Hwang, G.; Gamal El-Din, M.; Liu, Y. Development of nanosilver and multi-walled carbon nanotubes thin-film nanocomposite membrane for enhanced water treatment. *J. Membr. Sci.* **2012**, *394–395* (0), 37–48.
- (12) Tiraferri, A.; Kang, Y.; Giannelis, E. P.; Elimelech, M. Highly hydrophilic thin-film composite forward osmosis membranes functionalized with surface-tailored nanoparticles. *ACS Appl. Mater. Interfaces* **2012**, *4* (9), 5044–5053.
- (13) Potts, J. R.; Dreyer, D. R.; Bielawski, C. W.; Ruoff, R. S. Graphene-based polymer nanocomposites. *Polymer* **2011**, *52* (1), 5–25.
- (14) Kuilla, T.; Bhadra, S.; Yao, D.; Kim, N. H.; Bose, S.; Lee, J. H. Recent advances in graphene based polymer composites. *Prog. Polym. Sci.* **2010**, *35* (11), 1350–1375.
- (15) Ahmed, F.; Santos, C. M.; Vergara, R. A.; Tria, M. C.; Advincula, R.; Rodrigues, D. F. Antimicrobial applications of electroactive PVK-SWNT nanocomposites. *Environ. Sci. Technol.* **2012**, *46* (3), 1804–10.
- (16) Santos, C. M.; Mangadlao, J.; Ahmed, F.; Leon, A.; Advincula, R. C.; Rodrigues, D. F. Graphene nanocomposite for biomedical applications: Fabrication, antimicrobial and cytotoxic investigations. *Nanotechnology* **2012**, *23* (39), 395101.
- (17) Mejias Carpio, I. E.; Santos, C. M.; Wei, X.; Rodrigues, D. F. Toxicity of a polymer-graphene oxide composite against bacterial planktonic cells, biofilms, and mammalian cells. *Nanoscale* **2012**, *4* (15), 4746–56.
- (18) Santos, C. M.; Tria, M. C. R.; Vergara, R. A. M. V.; Ahmed, F.; Advincula, R. C.; Rodrigues, D. F. Antimicrobial graphene polymer (PVK-GO) nanocomposite films. *Chem. Commun.* **2011**, *47* (31), 8892–8894.
- (19) Hummers, W. S.; Offeman, R. E. Preparation of graphitic oxide. *J. Am. Chem. Soc.* **1958**, *80* (6), 1339–1339.
- (20) Deng, S.; Upadhyayula, V. K. K.; Smith, G. B.; Mitchell, M. C. Adsorption equilibrium and kinetics of microorganisms on single-wall carbon nanotubes. *IEEE Sens. J.* **2008**, *8*, 954–962.
- (21) Kang, S.; Herzberg, M.; Rodrigues, D. F.; Elimelech, M. Antibacterial effects of carbon nanotubes: Size does matter! *Langmuir* **2008**, *24* (13), 6409–6413.
- (22) Ellman, G. L. Tissue sulfhydryl groups. *Arch. Biochem. Biophys.* **1959**, *82* (1), 70–77.
- (23) Liu, S.; Zeng, T. H.; Hofmann, M.; Burcombe, E.; Wei, J.; Jiang, R.; Kong, J.; Chen, Y. Antibacterial activity of graphite, graphite oxide, graphene oxide, and reduced graphene oxide: membrane and oxidative stress. *ACS Nano* **2011**, *5* (9), 6971–6980.
- (24) Santos, C. M.; Tria, M. C. R.; Vergara, R. A. M. V.; Cui, K. M.; Pernites, R.; Advincula, R. C. Films of highly disperse electrodeposited poly(N-vinylcarbazole)-graphene oxide nanocomposites. *Macromol. Chem. Phys.* **2011**, *212* (21), 2371–2377.
- (25) Mejias Carpio, I. E.; Santos, C. M.; Wei, X.; Rodrigues, D. F. Toxicity of a polymer-graphene oxide composite against bacterial planktonic cells, biofilms, and mammalian cells. *Nanoscale* **2012**, *4* (15), 4746–4756.
- (26) Akhavan, O.; Ghaderi, E. *Escherichia coli* bacteria reduce graphene oxide to bactericidal graphene in a self-limiting manner. *Carbon* **2012**, *50* (5), 1853–1860.
- (27) Ahmed, F.; Santos, C. M.; Vergara, R. A. M. V.; Tria, M. C. R.; Advincula, R.; Rodrigues, D. F. Antimicrobial applications of electroactive PVK-SWNT nanocomposites. *Environ. Sci. Technol.* **2011**, *46* (3), 1804–1810.
- (28) Bao, Q.; Zhang, D.; Qi, P. Synthesis and characterization of silver nanoparticle and graphene oxide nanosheet composites as a bactericidal agent for water disinfection. *J. Colloid Interface Sci.* **2011**, *360* (2), 463–470.
- (29) Azam, A.; Ahmed, A. S.; Oves, M.; Khan, M. S.; Habib, S. S. Antimicrobial activity of metal oxide nanoparticles against Gram-positive and Gram-negative bacteria: A comparative study. *Int. J. Nanomed.* **2012**, *7* (1), 6003–6009.
- (30) Brady-Estevez, A. S.; Schnoor, M. H.; Vecitis, C. D.; Saleh, N. B.; Elimelech, M. Multiwalled carbon nanotube filter: Improving viral removal at low pressure. *Langmuir* **2010**, *26* (18), 14975–14982.

- (31) Brady-Estévez, A. S.; Kang, S.; Elimelech, M. A single-walled-carbon-nanotube filter for removal of viral and bacterial pathogens. *Small* **2007**, *4*, 481–484.
- (32) Santos, C. M.; Tria, M. C.; Vergara, R. A.; Ahmed, F.; Advincula, R. C.; Rodrigues, D. F. Antimicrobial graphene polymer (PVK-GO) nanocomposite films. *Chem. Commun.* **2011**, *47* (31), 8892–4.
- (33) Ahmed, F.; Santos, C. M.; Vergara, R. A.; Tria, M. C.; Advincula, R.; Rodrigues, D. F. Antimicrobial applications of electroactive PVK-SWNT nanocomposites. *Environ. Sci. Technol.* **2012**, *46* (3), 1804–10.
- (34) Gurunathan, S.; Han, J. W.; Dayem, A. A.; Eppakayala, V.; Kim, J. H. Oxidative stress-mediated antibacterial activity of graphene oxide and reduced graphene oxide in *Pseudomonas aeruginosa*. *Int. J. Nanomed.* **2012**, *7* (1), 5901–5914.
- (35) Santos, C. M.; Mangadlao, J.; Ahmed, F.; Leon, A.; Advincula, R. C.; Rodrigues, D. F. Graphene nanocomposite for biomedical applications: fabrication, antimicrobial and cytotoxic investigations. *Nanotechnology* **2012**, *23* (39), 395101.